UV laser micromachining of silicon, indium phosphide and lithium niobate for telecommunications applications

Jako Greuters and Nadeem Rizvi*

Exitech Limited
Oxford Industrial Park, Yarnton, Oxford, OX5 1QU, United Kingdom

ABSTRACT

The laser micromachining characteristics of indium phosphide, lithium niobate and silicon have been characterised using a 355nm neodymium vanadate laser and 193nm and 248nm excimer lasers. Etch rates for these materials are presented at the different laser wavelengths. High quality cutting of the three materials is demonstrated with the 355nm laser and an excimer laser mask projection method is subsequently used to micromachine precision V-grooves as fibre placement structures. Silicon microbenches, used for the integration of multiple-function devices, are also produced using the 355nm laser.

Keywords: laser micromachining; indium phosphide; lithium niobate; optical chips.

1. INTRODUCTION

Many of the developments currently being advanced in the telecommunications area mirror those which were made in the electronics sector more than thirty years ago, the overriding one of which is the aim of producing integrated devices with multiple optical functions onto a single chip [1,2] – the optical equivalent of the integrated circuit (IC). As in the case of ICs, such a development has many attractions in terms of speed of operation, increased performance, higher functionality and cost.

One of the legacies of the electronic era is that silicon (Si) has become the most intensely studied and developed material in manufacturing, and, as such, the processes for etching and processing it are highly mature. However, in the optical domain for telecommunications systems, silicon is often not the material of choice, even though it is still widely used. Other important materials which have emerged recently include indium phosphide (InP) and gallium arsenide (GaAs) (both used in optical modulators, semiconductor lasers and semiconductor amplifiers [3]) and lithium niobate ($LiNbO_3$) (used primarily in optical modulators [4]). All of these materials need to have new, robust production methods available to them if the aim of integrated optical devices is to be achieved since there is often incompatibility in the chemical (or other) etching techniques currently in existence. Also, present methods can also be somewhat restricted when addressing the new types of geometries and microstructures being considered for optical chips.

Laser micromachining offers many benefits as an alternative technique, such as:

- Single-stage 'dry' processing avoiding chemical or gaseous etching.
- Wide flexibility in features which can be produced in various 2D and 3D geometries.
- High precision and accuracy and ability to interface with CAD options.
- Relatively high speed.
- Ability to machine selectively different materials.
- Modest cost, both in capital equipment outlay and processing costs.

Since the use, handling and disposal of chemical or other consumables in 'conventional' etching systems is a serious issue, especially with increasingly stringent regulatory requirements, the absence of significant amounts of hazardous materials needed in laser micromachining is also of major benefit.

We present developments in laser micromachining as applied to telecommunications materials which demonstrate the feasibility of using laser-based methods in the manufacturing of integrated optical devices.

2. METHODOLOGY

The micromachining of Si, InP and $LiNbO_3$ was investigated with three laser wavelengths of 193nm, 248nm and 355nm, as detailed below.

Solid-State Laser Machining

The etch rates of Si, InP and $LiNbO_3$ (X-cut and Z-cut) were determined at a wavelength of 355nm by using a Lightwave Electronics diode-pumped $Nd-YVO_4$ laser operating at a wavelength of 355nm and a repetition rate of 10kHz. This laser was integrated into a micromachining workstation where the laser beam was focused using a 50mm focal length lens and the samples were positioned using air-bearing stages with a resolution of 100nm. Holes were statically drilled in the samples using different laser powers between 3.6W and 0.01W. The $LiNbO_3$ samples were drilled using 100 pulses and InP and Si with 20 pulses each. The depths of the blind holes were then measured using a high-resolution optical microscope with depth measurement capability and the single pulse etch rate calculated.

The machining of silicon was investigated using two different $Nd-YVO_4$ laser systems using:

(i) Lightwave Electronics laser, as described above, with a fluence of $110J/cm^2$, and the results are shown in figures 3-5;

(ii) Spectra Physics 532nm 'HIPPO' $Nd-YVO_4$ laser with a galvanometer scanner. The 15kHz laser beam was controlled by a Scanlab galvanometer scanner and focused onto the surface of the silicon wafer by a 100mm focal length. A fluence of $460J/cm^2$ was used and the result is shown in figure 6.

The $LiNbO_3$ wafer was cut at a fluence of $20J/cm^2$ and a cutting rate of 0.0625mm/sec was achieved.

The InP samples were machined using a Spectra Physics YHP laser operating at a wavelength of 355nm and a repetition rate of 5kHz. The laser beam was focused with a lens of 106mm focal length lens and the sample handled with 1µm resolution stages. At a fluence of $14J/cm^2$ a total cut speed of 0.008mm/sec was achieved for a 350µm thick wafer, as shown in figure 7.

In the cases of Si and $LiNbO_3$ cutting, nitrogen was used as an assist gas and was applied to the samples by a gas nozzle.

In all three cases (Si, $LiNbO_3$ and InP), a PVA-based debris protective coating was used on the samples during the laser machining and subsequently removed.

Excimer Laser Micromachining

The etch rates of $LiNbO_3$ X-cut and Z-cut were determined by using an Exitech S7000 UV micromachining tool. The system was equipped with a Lambda Physik LPX210 operating at a wavelength of 248nm and translation stages with a 1µm resolution. Beam homogenisers illuminated the rectangular mask with a uniform beam and a projection lens (x10, 0.2NA, 248nm) was used to image the mask onto the samples. The samples were exposed to 100 laser pulses at fluences ranging from $0.01J/cm^2$ to $7J/cm^2$. The depth of the ablated holes were measured on an optical microscope and the etch rate calculated.

Using the etch rate data, the numbers of pulses required to machine passive fibre alignment V-grooves to the appropriate depth were calculated and the V-grooves machined into X-cut and Z-cut $LiNbO_3$ on the Exitech S7000 micromachining tool. The V-grooves were machined using the well-established workpiece dragging technique [5,6] at a fluence of $4J/cm^2$, a total machining speed of 0.01mm/sec and a laser repetition rate of 100Hz. Nitrogen gas assist and debris protection coating was used on all the $LiNbO_3$ samples.

3. SOLID-STATE LASER MICROMACHINING

3.1 Etch Rate at 355nm

The etch rates of Si, InP and LiNbO$_3$ at 355nm are shown in figure 1. It can be seen that the etch rates of both X-cut and Z-cut LiNbO$_3$ are essentially identical, in contrast to the etching behaviour of the two crystal orientations [7].
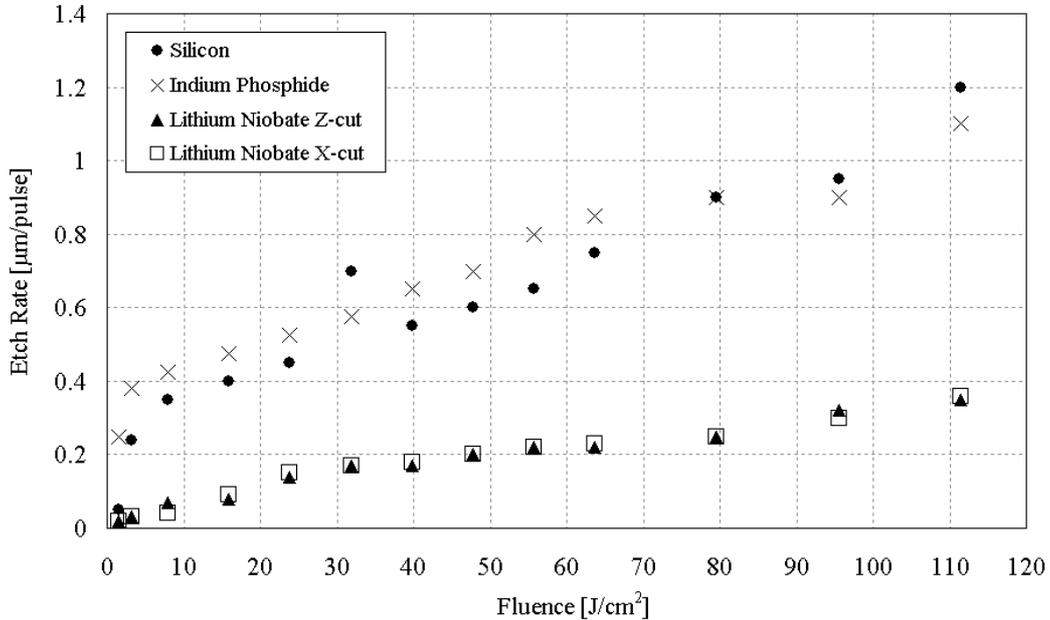

Figure 1: Etch rates for Si, InP and LiNbO$_3$ (x-cut and z-cut) at 355nm.

The etch rates of both InP and Si are similar, at around 1μm per pulse for an exposure fluence of around 100J/cm^2. The etch rate of LiNbO$_3$ is typically around 0.2-0.3μm per pulse which corresponds to around 1mm/sec for a 5kHz laser.

3.2 Laser Machining at 355nm

As seen in figure 1, there is no difference in the material removal rates of X-cut and Z-cut LiNbO$_3$. No qualitative difference in the machining quality of the two orientations of samples was found either and so only the X-cut result is shown in figure 2 (although a comparison between the laser machining quality between X-cut and Z-cut is shown in figure 9).

As can be seen from figure 2, the LiNbO$_3$ sample machined with extremely high quality and the straightness and cleanliness of the cut edges are clearly evident. The small defects which can be seen in the extracted piece of wafer were due to mechanical handling after the sample had been laser machined. No microcracking was observed on the laser-cut pieces under examination with a high magnification optical microscope or scanning electron microscope.

Laser machining of the kind demonstrated in figure 2 opens up possibilities for highly precise and efficient chip extraction from sample wafers with minimal material loss due to the actual cut width and, consequently, the ability to pack more chips onto a single wafer, thereby increasing material use.

Figure 3 shows a silicon sample machined using the Lightwave Electronics 355nm laser and a static laser beam (i.e. with moving sample stages). A laser fluence of 110J/cm^2 was used and 250 passes at 16.66mm/sec were made to cut

through the 350µm thick wafer, giving an total cutting speed of 0.066mm/sec. The overall quality of the cut edges, lack of chipping, lack of thermal damage and absence redeposited material are clearly observed.
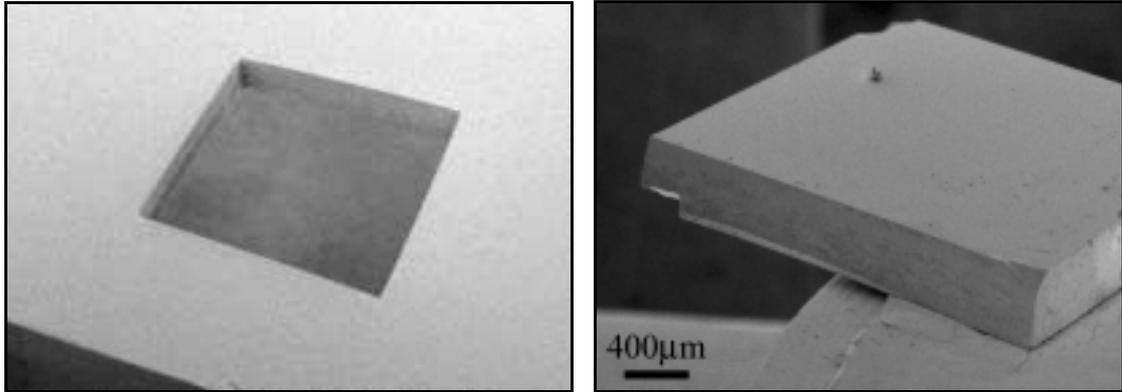

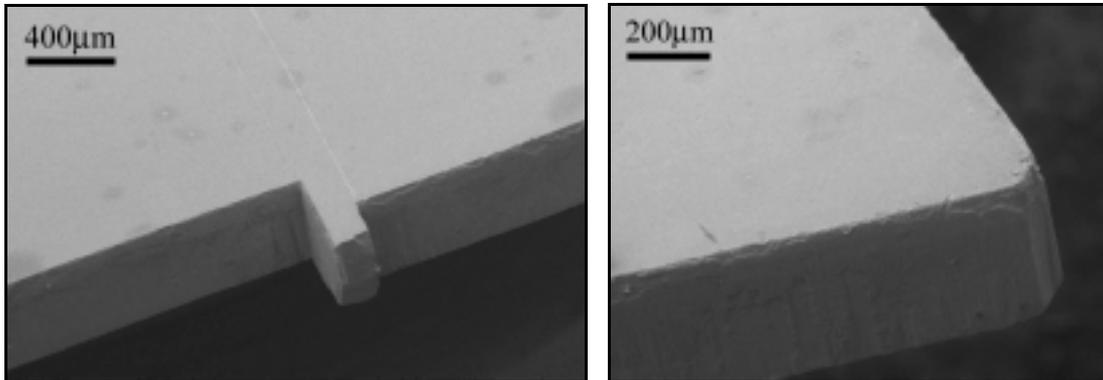Figure 2. LiNbO$_3$ x-cut crystal cut with 355nm Nd-YVO$_4$ laser

Figure 3. Silicon wafer cut with 355nm Nd-YVO$_4$ laser.

Using the same set-up as for the results in figure 3 and with optimised cutting parameters, a demonstrator silicon microbench was machined, as shown in figure 4. The inherent precision in the laser-machined samples means that the two parts of the microbench align very easily and with high precision. The 'closed' size of the microbench was 5mm x 6mm and laser-made fibre positioning slots can be seen on the surface of the microbenches.
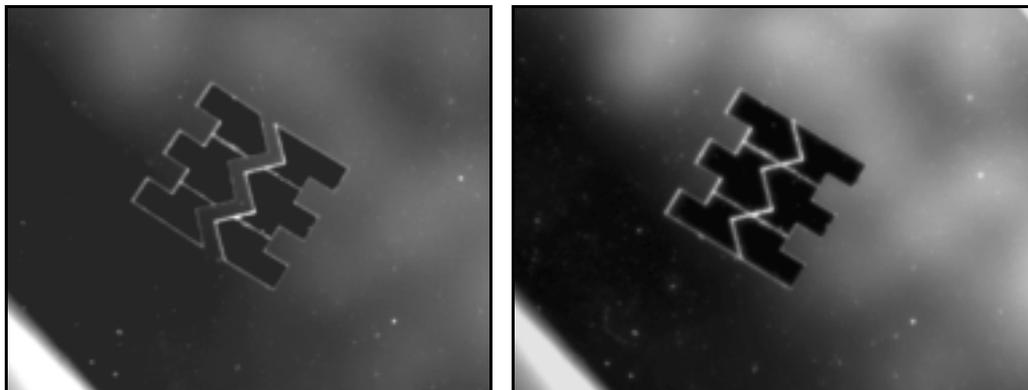

Figure 4. Silicon microbenches machined using a 355nm laser, in 'open' (separated) and 'closed' (aligned) positions.

Such microbenches are important in the passive alignment in optical systems, for example in the coupling of fibres to other devices, and also serve as a platform for the integration of active and passive components such as amplifiers, switches, modulators and filters.

A magnified view of one of the 'teeth' of the silicon microbench is shown in figure 5, which shows the sharpness of machining and high quality achieved.
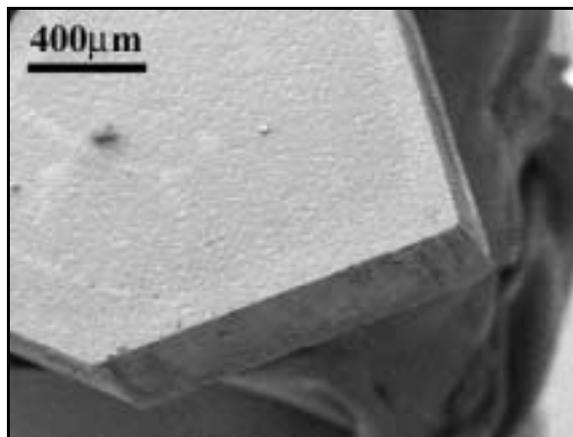

Figure 5. SEM of 'tooth' of silicon microbench shown in figure 4.

An alternative method of cutting silicon, namely using a galvanometer-scanned beam on a static sample, was used at a laser wavelength of 532nm and the cut edge on a 525μm thick silicon wafer is shown in figure 6. A fluence of 460J/cm^2 was used and 250 passes were made at a speed of 500mm/sec to cut the sample, giving a total cutting speed of 2mm/sec.

A distinct improvement was seen, as shown in figure 6, in the smoothness of the cut face and the quality of the edge. This was largely attributed to the much higher beam speed over the sample which was permitted by the use of the scanner and this helped in minimising the build-up of thermal effects and led to the improvement in machining quality.
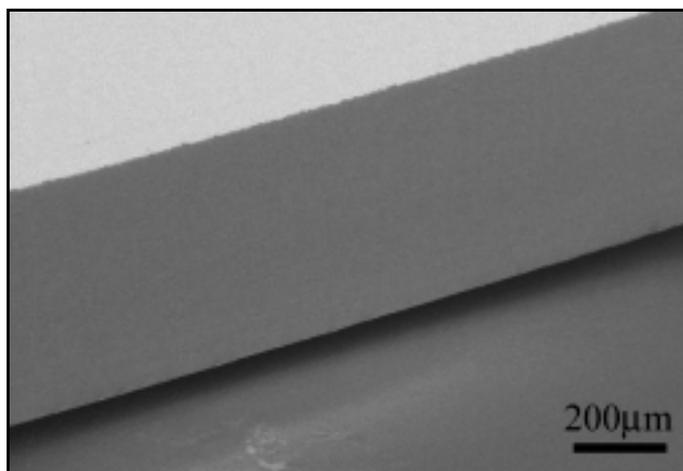

Figure 6. SEM of cut face of silicon machined using a scanned beam from 532nm Nd-YVO$_4$ laser.

Figure 7 shows the high quality cutting of InP. A fluence of 14J/cm^2 was used and 200 passes were made at a speed of 1.6mm/sec to achieve the cuts.
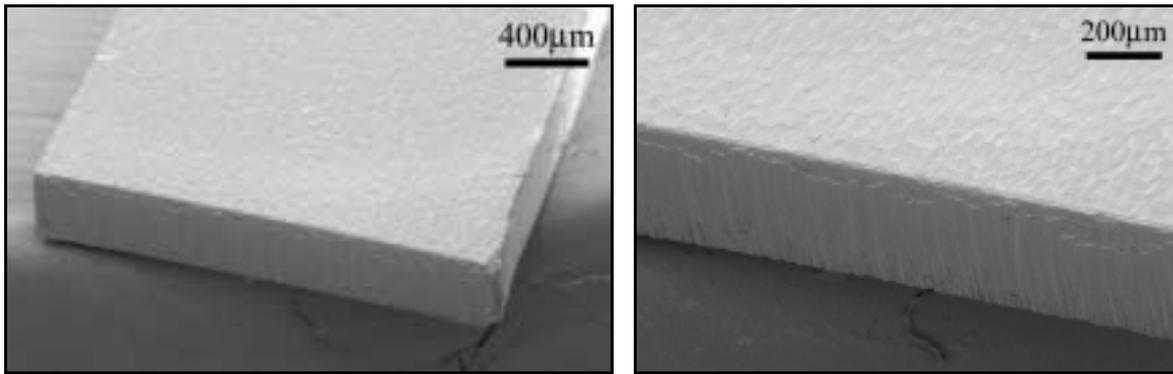
Figure 7. SEMs of InP chips cut with 355nm Nd-YVO$_4$ laser.

The clean and high quality machining is again clearly evident. In the same manner as with the LiNbO$_3$ chips, this provides an effective demonstration of chip extraction from InP wafers.

4. EXCIMER LASER MICROMACHINING

The etch rates of lithium niobate were measured at two excimer laser wavelengths and are shown in figure 8. It can be seen that, as in the case of 355nm machining shown in figure 1, there is no significant difference in the etch rates of X-cut or Z-cut samples at either wavelength. This again highlights the flexibility in the use of laser machining in that crystal orientation can be ignored when laser machining lithium niobate.
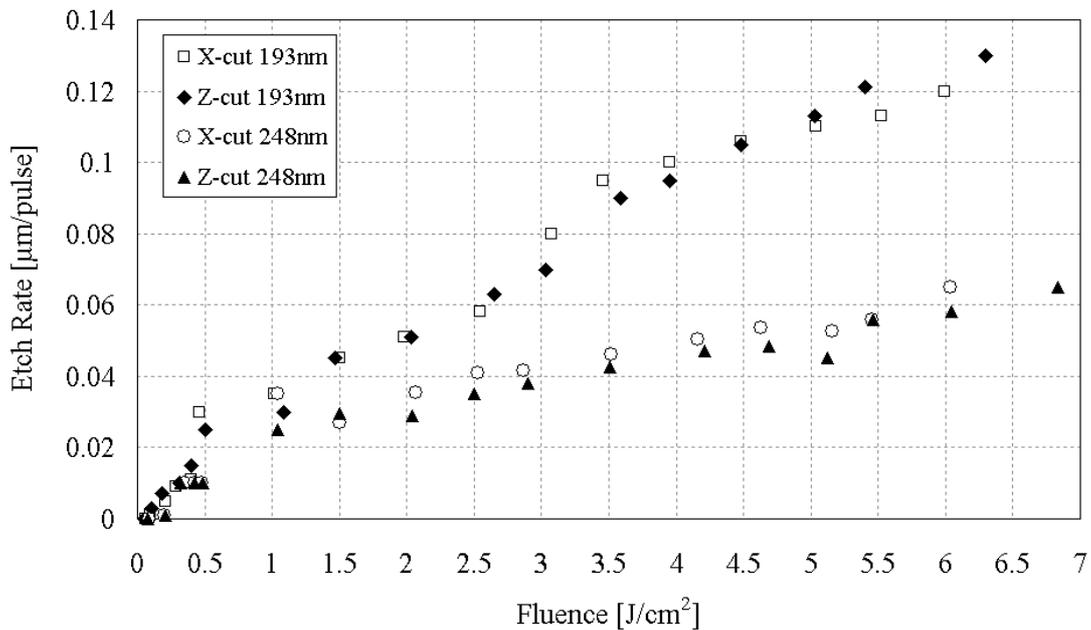

Figure 8. Etch rates of LiNbO$_3$ at excimer laser wavelengths of 193nm and 248nm.

The etch rates for the lithium niobate samples were used to calculate the required conditions for the micromachining of V-grooves using a 248nm laser. V-grooves in both X-cut and Z-cut samples were produced by the workpiece dragging method using a triangular mask [4] and the results are shown in figure 9. Smooth sidewalls and sharp edges

can be noticed which enables the fibre to sit reproducibly in the V-grooves. Figure 9 again shows the insensitivity of the laser machining to the crystal orientation, as opposed to the results obtained with reactive-ion etching [7].
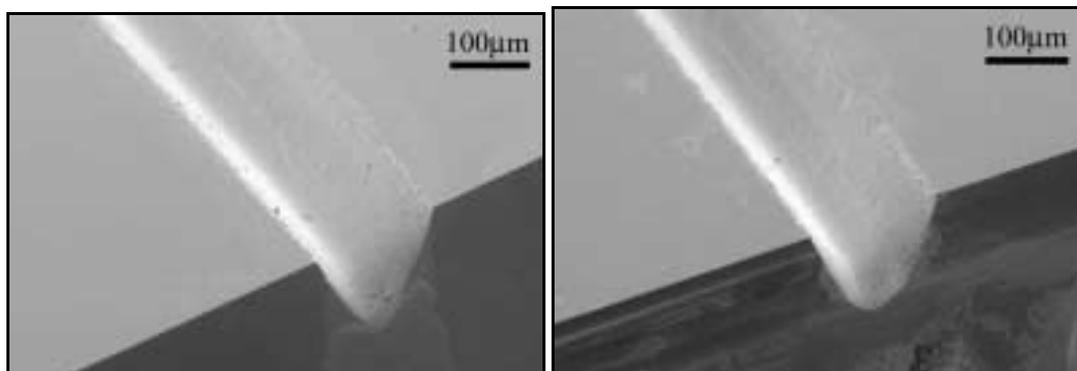

Figure 9. SEMs of V-grooves machined in LiNbO$_3$ X-cut (left) and Z-cut (right) at 248nm.

Having produced the V-grooves shown in figure 9, preliminary fibre positioning and alignment tests were initiated, and the seating of a standard fibre (ϕ125μm cladding) in the V-grooves is shown in figure 10. The reproducibility of the fibre seating was tested by observing the position of the centre of the fibre with respect to the sample surface but more quantitative work is now underway to measure the coupling efficiency and reproducibility of the fibre positioning.
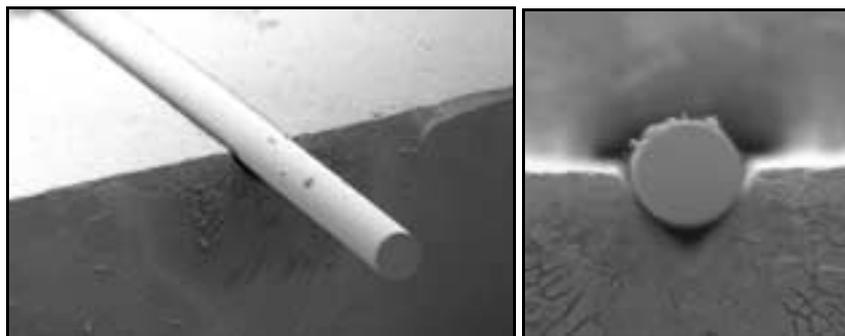

Figure 10. SEM of optical fibre positioned in laser-machined V-groove in LiNbO$_3$.

A common construction in many optical devices involves the positioning of an optical fibre to couple light into or out of another waveguide. In the case of optical modulators, this waveguide is most commonly a buried waveguide made by diffusion methods [8]. To demonstrate the feasibility of laser machining a modulator device with this form of fibre coupling, a 5mm x 5mm chip of lithium niobate was extracted from a 2-inch wafer using a 355nm laser. A V-groove for a standard telecommunications fibre (Corning SMF28) was then machined into the LiNbO$_3$ chip using a 248nm excimer laser, following which an orthogonal rectangular cross-section trench was machined in the sample (using 248nm mask projection). The resulting structure is shown in figure 11.

The rectangular trench is used to define the face of the waveguide to which the fibre has to couple to and it also enables the core of the fibre to be at the correct height to match the buried waveguide in the sample. Although in the case shown in figure 11 there was no waveguide present in the sample, the capability of laser machining to produce such structures has clearly been demonstrated.

The flexibility in the laser machining process allows the angle of the waveguide facet (i.e. the angle of the sidewall of the rectangular trench) to be controlled such that non-normal facets can be produced.
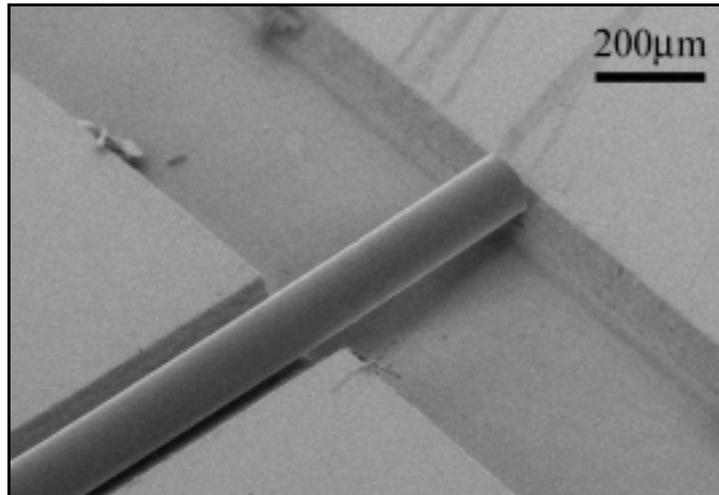
Figure 11. SEM of LiNbO$_3$ optical fibre positioning and coupling structure

5. SUMMARY

The characteristics of laser machining of three important optical materials used in the telecommunications industry have been investigated. It was found that laser machining of lithium niobate in its two most common crystal orientations was identical and that, contrary to conventional etching methods, there was no sensitivity to the crystal orientation for laser micromachining. A combination of UV solid-state and excimer lasers has also been used to demonstrate the production of a passive fibre and waveguide alignment feature with applicability to a wide range of photonics devices

6. AKNOWLEDGEMENTS

7. REFERENCES

1. E.J. Murphy, Ed., Integrated Optical Circuits and Components: Design and Applications, Marcel Dekker, New York, 1999.
2. G. Ferris Lipscomb, M. Stiller, "Planar waveguide integration adds flexibility, improves performance", WDM solutions, p75, October 2001.
3. *Indium Phosphide & Related Materials (Special Issue)* Jpn. J. Appl. Phys. Vol.38, *Part 1, No.2B,* 1999
4. E. L. Wooten, et al., A review of lithium niobate modulators for fiber-optic communication systems, IEEE J.of Selected Topics in Quantum Electronics, **6**, 1, 69-82, 2000.
5. E.C. Harvey, and P.T.Rumsby, "Fabrication techniques and their application to produce novel micromachined structures and devices using excimer laser projection" in *Micromachining and Microfabrication Process Technology III*, Proc. SPIE **3223**, 26-33 (1997)
6. N. H. Rizvi, "Production of novel 3D microstructures using excimer laser mask projection techniques", in Design Test and Microfabrication of MEMS and MOEMS, Proc. SPIE 3680, 546-552 (1999)
7. S. Winnall, S. Winterbaum, "Lithium niobate reactive ion etching", http://dsto.hearne.com.au/cgi-bin/extract.pl?DSTO-TN-0291
8. R.V. Schmidt, I.P. Kaminow, "Metal-diffused optical waveguides in LiNbO$_3$" , Appl. Phys. Lett., **25**, No 8, 458-460, 1974.

 * n.rizvi@exitech.co.uk; Phone 44 1865 290400; Fax 44 1865 290401; http://www.exitech.co.uk